Technical University of Denmark

DTU

Modelling the Effect of Exercise on Insulin Pharmacokinetics in "Continuous Subcutaneous Insulin Infusion" Treated Type 1 Diabetes Patients

Duun-Henriksen, Anne Katrine; Juhl, Rune; Schmidt, Signe; Nørgaard, Kirsten; Madsen, Henrik

Publication date:
2013

Document Version
Publisher's PDF, also known as Version of record

DTU Compute Technical Report-2013-13

Modelling the Effect of Exercise on Insulin Pharmacokinetics in "Continuous Subcutaneous Insulin Infusion" Treated Type 1 Diabetes Patients

Anne Katrine Duun-Henriksen[a,*], **Rune Juhl**[a], **Signe Schmidt**[b], **Kirsten Nørgaard**[b], **Henrik Madsen**[a]

[a] Department of Applied Mathematics and Computer Science, Technical University of Denmark
[b] Department of Endocrinology, Hvidovre University Hospital, Denmark

Abstract

Introduction: The artificial pancreas is believed to ease the burden of constant management of type 1 diabetes for the patients substantially. An important aspect of the artificial pancreas development is the mathematical models used for control, prediction or simulation. A major challenge to the realization of the artificial pancreas is the effect of exercise on the insulin and plasma glucose dynamics. In this report, we take the first step towards a population model of exercise effects in type 1 diabetes. We focus on the effect on the insulin pharmacokinetics in continuous subcutaneous insulin infusion (CSII) treated patients by modelling the absorption rate as a function of exercise. **Methods**: Three models are estimated from 17 data sequences. All of them are based on a linear three-compartment base model. The models are based on stochastic differential equations to allow noise to enter the dynamics. In the first model, the insulin absorption rate parameter is replaced by a random walk. In the second model, the relationship between the absorption rate and exercise is modelled as a linear dependency, while in the third model this linear relationship depends on the intensity. A Lamperti transformation is used to ensure non-negative state values. A special focus is put on the structural identifiability of the base model, while the posterior identifiability is checked for all models from the conditional likelihood profiles. **Results**: The first model is disregarded due to the small number of observations during the exercise bout. From likelihood-ratio tests and information criteria, the third model is appointed as the best model to model the relationship between exercise and the insulin absorption. The posterior identifiability check showed that it was not possible to identify the variance of the measurement variance. **Conclusion**: A model to predict the insulin appearance in plasma during exercise in CSII treated patients is identified. Further clinical studies are needed to confirm the increase in insulin plasma concentration during exercise in type 1 diabetes patients. These studies should include dense sampling to allow for a fully data driven identification of an appropriate model.

Keywords: Continuous subcutaneous insulin infusion, Stochastic differential equations, Population models, Exercise in type 1 diabetes, Lamperti transformation

* *Contact author:akdu@dtu.dk*
Technical University of Denmark
Department of Applied Mathematics and Computer Science
Matematiktorvet, Building 322, DK-2800 Kgs. Lyngby, Denmark
Tel: +45 4525 3399, email: akdu@dtu.dk

1 Introduction

The treatment of type 1 diabetes opposes a major challenge on the patients and their health care providers. Thus many initiatives are investigated to ease the burden and to simplify the daily management of the disease. A promising approach is the so-called *artificial pancreas* consisting of an insulin pump delivering insulin continuously, a continuous glucose monitor (CGM) and a control algorithm to regulate the insulin infusion automatically based on feedback from the CGM. The insulin pump and the CGM are commercially available today, but the patients are required to regulate the pump themselves several times daily. Hence, the connection of the pump and CGM via a control algorithm are believed to ease the management of type 1 diabetes for the patients substantially [1].

Currently, the research activities within the artificial pancreas area is rapidly developing due to an increasing number of researchers and technological advances. One of the main challenges for an artificial pancreas is the management of the plasma glucose level during and after exercise. The exercise effects on the blood glucose level are adverse and depends on intensity, duration, timing related to meals and insulin boluses, and type of activity [31].

Mathematical models resembling the dynamics of insulin-glucose system are important tools in the development of control algorithms for the artificial pancreas. *Virtual* type 1 diabetes patients enable the researchers to test various treatment scenarios and identify the most promising algorithms prior to expensive and time-consuming clinical studies.

Until now several models have been suggested to mimic the dynamic relation between exogenous insulin and blood glucose in type 1 diabetes. They include the transport of glucose from meals to the plasma [34, 7, 15]. Few models have dealt with the effect of exercise on the insulin sensitivity and blood glucose level [5, 6, 33, 18, 13, 8, 26].

Clinical studies investigating the effects of exercise in type 1 diabetes have mainly focused on the effects on changes in plasma glucose [31]. Several studies have however shown a significant increase in insulin absorption during physical activity in type 1 diabetes patients [11, 29, 30, 36, 3, 28, 27]. The cause of this increase is not clarified, but increasing blood flow or temperature in the peripheral area of the body could be the cause. In [2], they show that a hot bath and local massage at the injection site increase the speed of the insulin absorption after a subcutaneous injection. To our knowledge, the increase related to exercise has not been investigated from a pharmacokinetic modelling perspective. However, to understand the glucose dynamics during exercise it is necessary to determine whether the increase is caused by changes in insulin pharmacokinetic or pharmacodynamic parameters or if it is unrelated to the insulin concentration.

In this report, a model of the effects of exercise on the insulin pharmacokinetics is developed. We identify a proper population model for the effect of exercise on the subcutaneous absorption of insulin delivered continuously by an insulin pump. The model could potentially be implemented into a simulation model of the insulin-glucose dynamics.

We employ stochastic differential equations (SDEs) instead of the traditional ordinary differential equations (ODEs). In SDEs, the residual noise is split into a diffusion term and a normally distributed and uncorrelated measurement noise. This helps to ensure that the residuals are independent as required by standard statistical model validation tools. Furthermore, the noise is allowed to enter the system to account for the inherent uncertainties in all models of physiological systems. Finally, SDEs provide us with a method to pinpoint model deficiencies and to suggest how to extent the model to capture the relevant behavior [17, 32].

The structure of the paper is the following: In Section 2, the clinical data set is described. Then, in Section 3 the models and methods are described including a identifiability check. In Section 4, the results are presented. Section 5 presents a discussion of the study. Finally, in Section 6 the conclusions are stated.

2 Data

The insulin data for this study originates from a clinical study on 12 subjects with type 1 diabetes treated with continuous subcutaneous insulin infusion (CSII). The insulin pump was placed in the subcutaneous layer in either the abdominal or gluteal area. The purpose of the clinical study was to evaluate the effect of insulin boluses, meals and exercise on the plasma glucose level [27, 10]. Beside plasma glucose, insulin plasma levels were analysed. The insulin type was insulin aspart *Novorapid* - a fast acting insulin type.

Each patient went through two study days separated by at least three weeks. A study day consisted of a two hour stabilization period followed by three events separated by 150 min. The three event types were meals, insulin boluses and a 20 minutes-run on a treadmill at a predetermined heart rate (HR). Not two of the total 24 study days were identical as the order of events where different from study day to study day. The predetermined HR corresponded to either mild exercise with a HR equal to 50% of (maximum HR - resting HR) + resting HR or moderate exercise with a HR equal to 75% of (maximum HR - resting HR) + resting HR.

Insulin observations were sampled at a non-equidistantly sampling scheme with higher frequency just after each event and analysed with a LOCI technology. For each study day a data sequence was obtained. In some of the data sequences the plasma insulin concentration was not in steady-state during the stabilization period prior to the first event. Thus we removed data sequences with at min-max range $> 5mU/L$ during the stabilization period to ease the model estimation. Six of the study days included exercise on mild level, eight of them included exercise on moderate level, while three of them did not include exercise.

3 Methods

Our interest is to model population characteristics related to exercise. To identify a proper model taking into account the inter-individual variability we use a population modelling approach. This type of models is build as hierarchical models where the parameters are estimated in a two-stage manner. Individual parameters are modelled as a combination of fixed population effects and random individual effects as seen in (1):

$$\theta_i = h(\theta_{pop}, Z_i) \cdot exp(\eta_i) \tag{1}$$

Here θ_i is the parameter value for individual i, $h(\cdot)$ is a known function, θ_{pop} is the overall population parameter (fixed effect), Z_i are covariates (age, weight, gender etc.), and $\eta_i \sim N(0, \Omega)$ is the individual random effect. In the first stage, the random effects, η_i's, are estimated for each individual. The fixed effect parameters, θ_{pop}, are estimated in the second stage with the entire data set from an approximate population likelihood function [32].

In the single-subject modeling case, the R-package CTSM-R (Continuous Time Stochastic Modelling in R) can be used to identify SDE models [9]. However, currently CTSM cannot handle population models. Thus as a part of this study, a prototype of an population modelling extension to CTSM was developed.

The modelling procedure is the following. First, a base model is estimated without any exercise effects. A number of extensions to this model are then estimated to identify the most appropriate model of the exercise effects.

3.1 The Base Model

A linear three-compartment ODE model is used as basis to describe the pharmacokinetics of subcutaneous infused insulin in a single subject as suggested by Wilinska et al. [34]. The model is illustrated in Figure 1.

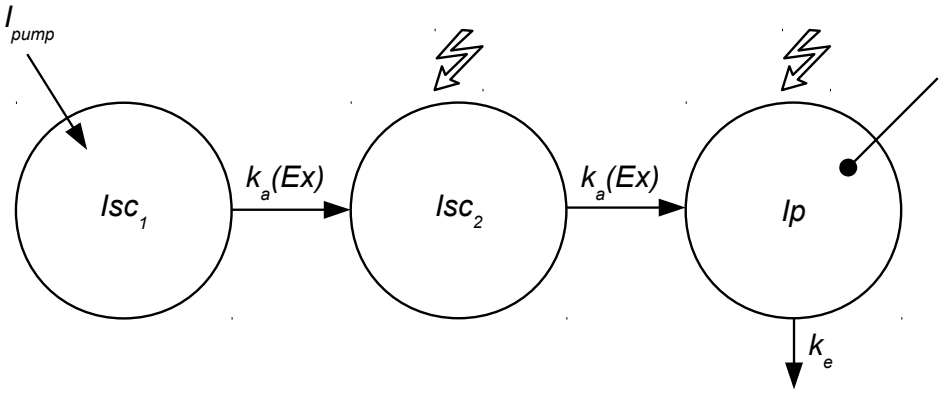

Figure 1: *Illustration of the three-compartment model describing the pharmacokinetics of insulin delivered continuously from an insulin pump. Lightnings indicate diffusion terms.*

The absorption is characterized by an identical rate parameter, k_a between all three compartments. Two compartments are affected by diffusion.

The total SDE model is presented on state-space form in (2) and (3):

$$d\begin{bmatrix} Isc_1 \\ Isc_2 \\ Ip \end{bmatrix} = \begin{bmatrix} (I_{pump} - k_a \cdot Isc_1)dt \\ (k_a \cdot Isc_1 - k_a \cdot Isc_2)dt + \sigma_{Isc} d\omega_{Isc} \\ (\frac{k_a}{V_I} \cdot Isc_2 - k_e \cdot I_p)dt + \sigma_{Ip} d\omega_{Ip} \end{bmatrix} \tag{2}$$

where Isc_1 [mU] and Isc_2 [mU] represent the subcutaneous layer and deeper tissues, respectively, and Ip [mU/L] represents plasma. I_{pump} is the input from the pump [mU/min]. k_a [min^{-1}] is the absorption rate and k_e [min^{-1}] is the clearance rate of insulin from plasma. V_I is the volume of distribution [L]. σ_{Isc} and σ_{Ip} are diffusion scaling parameters. ω_{Isc} and ω_{Ip} are Wiener processes with independent Gaussian increments [19]. They constitute the diffusion terms entering the system.

The observations are linked to the system with the observation equation:

$$log(y_k) = log(Ip_k) + e_k \tag{3}$$

where y_k are the discrete observations of plasma insulin concentration and $e_k \sim N(0, \xi)$ is the measurement noise.

To introduce the hierarchical structure of the model, the parameters are specified for each individual as in (1). The individual initial values and parameters are:

$$\theta_i = \begin{bmatrix} Isc_{1_0 i} \\ Isc_{2_0 i} \\ Ip_{0i} \\ k_{ai} \\ k_{ei} \\ V_{Ii} \\ \sigma_{Isci} \\ \sigma_{Ipi} \\ \xi_i \end{bmatrix} = \begin{bmatrix} Isc_{1_0} \cdot exp(\eta_{i1}) \\ Isc_{2_0} \cdot exp(\eta_{i1}) \\ Ip_{0i} \\ k_a \cdot exp(\eta_{i_2}) \\ k_e \cdot exp(\eta_{i3}) \\ V_I \cdot weight_i \\ \sigma_{Isc} \\ \sigma_{Ip} \\ \xi \end{bmatrix} \tag{4}$$

where $weight_i$ is the body weight [kg] of individual i. $\eta_{i1}, \eta_{i2}, \eta_{i3} \sim N(0, \Omega)$ where Ω is a diagonal matrix with three element: Ω_{Isc}, Ω_{ka}, and Ω_{ke}. The measurement noise is modelled as an exponential error

to approximate the assumption of a proportional measurement error. Furthermore, the variance of the measurement noise, ξ is parameterized as $\xi = S_{min} + S$, where S_{min} is fixed to the a reasonable minimum variance and S is estimated. The value of S_{min} is found from a mean value of estimated %CVs (coefficient of variation) for the relevant concentration range in [25].

As seen in (2), Ip is affected by additive diffusion and thus negative values can be obtained. This is problematic, first of all because it is non-physiological, but also due to the structure of the observation equation in (3) which cannot be computed when $Ip_k < 0$. Instead, we use a multiplicative state-dependent diffusion term for Ip to ensure that the state is strictly positive:

$$dIp_i = \left(\frac{k_{ai}}{V_{Ii}} \cdot Isc_{2i} - k_{ei} \cdot Ip_i \right) dt + \sigma_{Ip_i} Ip_i \, d\omega_{Ip} \tag{5}$$

3.2 Lamperti State Transformation

As CTSM cannot handle state-dependent multiplicative diffusion we transform the state, Ip_i into a space where this multiplicative noise becomes additive, z_{Ip_i}. This can be done by a *Lamperti* transformation. A description of the derivation of the Lamperti transformation is out of the scope of this report. However, details about the transformation can be found in [14, 24, 23, 4, 22]. We consider a general system equation:

$$dx_t = f(x_t, t, u_t)dt + \sigma_{x_t} x_t d\omega_{x_t} \tag{6}$$

where x_t represents the states and u_t represents the inputs to the system. We can then choose a transformed equation, z_t as:

$$z_t = \psi(x_t) = \int \frac{1}{s} ds \Big|_{s=x_t} = \log(x_t) \tag{7}$$

According to the theory behind the Lamperti transformation, z_t is governed by:

$$dz_t = \left(\frac{f(\exp(z_t), t)}{\exp(z_t)} - \frac{1}{2}\sigma_{x_t}^2 \right) dt + \sigma_{x_t} d\omega_{z_t} \tag{8}$$

As seen, the transformation eliminates the state-dependent diffusion term from x_t. Repeating this procedure for Ip_i, we get the transformed state, z_{Ip_i}:

$$dz_{Ip_i} = \left(\frac{\frac{k_{ai}}{V_{Ii}} \cdot Isc_{2i} - k_{ei} \cdot exp(z_{Ip_i})}{exp(z_{Ip_i})} + \frac{1}{2}\sigma_{Ip_i}^2 \right) dt + \sigma_{Ip_i} d\omega_{z_{Ip}} \tag{9}$$

The observation equation in (3) simply transforms into:

$$\log(y_{ki}) = z_{Ip_i k} + e_{ki} \tag{10}$$

For technical reasons, we used the following observation equation for the rest of the study:

$$y_{ki} = exp(z_{Ip_ik}) + e_{ki} \tag{11}$$

The Lamperti-transformation ensures that the diffusion term is additive while the parameters are the same as in the original model in (5) and (3).

3.3 Structural Identifiability

Prior to parameter estimation, the identifiability of the model is checked to make sure that we can find a reliable estimate of the model. Two types of identifiability exists: Structural identifiability and identifiability related to the experimental conditions. In the following, the structural identifiability of the base model for a single subject is investigated. For the sake of simplicity, the observation equation is considered to be continuous, but the result applies to the discrete observation equation as well. First, the state-space model in (2) is rewritten into the general form for linear state-space models:

$$\begin{aligned} dx_t &= (Ax_t + Bu_t)\,dt + \Sigma d\omega_t & (12)\\ y_t &= Cx_t + e_t & (13) \end{aligned}$$

For the base model, the matrices A, B, C and Σ are specified as:

$$\begin{aligned} A &= \begin{bmatrix} -k_a & 0 & 0 \\ k_a & -k_a & 0 \\ 0 & \frac{k_a}{V_I} & -k_e \end{bmatrix} \quad B = \begin{bmatrix} 1 \\ 0 \\ 0 \end{bmatrix} \\ C &= \begin{bmatrix} 0 & 0 & 1 \end{bmatrix} \qquad\qquad \Sigma = \begin{bmatrix} 0 & 0 & 0 \\ 0 & \sigma_{Isc} & 0 \\ 0 & 0 & \sigma_{Ip} \end{bmatrix} \end{aligned} \tag{14}$$

To determine whether the model is structural identifiable, the transfer functions, G_p and H_p are used. G_p and H_p describe the relationship between the input and output, and the noise and output, respectively:

$$y_t = G_p \cdot u_t + H_p\epsilon_t \tag{15}$$

where ϵ_t is the part of the output that cannot be predicted exactly (the difference between the observed and estimated concentration). First, we consider the deterministic part of the model and hence G_p, which can be found from the following the relationship:

$$G_p = C\,(pI - A)^{-1}\,B \tag{16}$$

We are able to observe G_p from u_t and y_t in the following form:

$$G_p = \frac{b_j p^j + b_{j-1}p^{j-1} + ...b_0}{a_l p^l + a_{l-1}p^{l-1} + ...a_0} \tag{17}$$

where $a_l = 1$. In our case $j = 0$ and $l = 3$. From (16) and (14) we find:

$$G_p = \frac{\frac{k_a^2}{V_I}}{(p + k_a)^2 (p + k_e)} \tag{18}$$

If the model is structural identifiable we are able to identify k_a, k_e, and V_I from a_0, a_1, a_2, and b_0 in (17). We can obtain four equations from (17) to determine k_a, k_e, and V_I from (17) and (18):

$$\frac{b_0}{a_2 p^2 + a_1 p^1 + a_0} = \frac{\frac{k_a^2}{V_I}}{(p + k_a)^2 (p + k_e)} \Rightarrow \tag{19}$$

$$\begin{array}{rclrcl} b_0 & = & \frac{k_a^2}{V_I} & a_0 & = & k_a^2 k_e \\ a_1 & = & k_a (k_a + 2k_e) & a_2 & = & 2k_a + k_e \end{array} \tag{20}$$

Four equations and only three parameters is an overdetermined system. While there is no guarantee for all equations to be fulfilled there will be a solution in some appropriate norm (L2). Thus the system is structurally identifiable. Regarding the identifiability of the noise parameters, the analytical solution is cumbersome. However, the following holds for the number of identifiable noise parameters:

$$\#\, of\ ident.\, noise\, parameters \ \leq nm + m(m+1)/2 \tag{21}$$

where n is the order of the system, in our case $n = 3$ and m is the number of outputs; in our case $m = 1$. Thus we can identify at most four noise parameters. The model is specified with only three noise parameters as seen in (2) and (3). For more details about structural identifiability see [20]. Whether the base model is identifiable from the experimental conditions is checked in a posterior manner from the estimated conditional likelihood profiles for each parameter – see Section 4.

3.4 Exercise Effects

The aim of the study is to investigate the effect of exercise on the absorption rate parameter, k_a. To include this effect, three approaches are investigated. The first one exploits the ability of SDEs to track parameter variation. The parameter, k_a is modelled as a random walk to investigate if the absorption rate increases during exercise:

$$dk_a = 0\, dt + \sigma_{k_a} d\omega_3 \tag{22}$$

where σ_{k_a} is a scaling diffusion parameter. The model with this specification is named *Model A*

In the second approach, we specify k_a as:

$$k_a = \bar{k}_a + \alpha \cdot Ex \tag{23}$$

where $\bar{k}_a$ represents the basal rate and α determines the effect of exercise, Ex. Ex is specified as a vector with the value 0 when the patient is not exercising and the value 1 during exercise. This model is named *Model B*.

With the third approach we take into account the fact that the subjects exercised on two different intensity levels. Thus we extend (23) to:

$$k_a = \bar{k}_a + \alpha_{mild} \cdot Ex_{mild} + \alpha_{moderate} \cdot Ex_{moderate} \tag{24}$$

Here, α_{mild} and $\alpha_{moderate}$ determines the effect of mild and moderate exercise, respectively. Ex_{mild} and $Ex_{moderate}$ are specified as Ex just for each of the two levels. This model is named *Model C*.

In all cases the model becomes non-linear. Hence, the identifiability check presented earlier cannot be used for the extended models. However, the posterior check is performed for these models as well.

3.5 Parameter Estimation with CTSM

The parameters are estimated by minimising the likelihood function resulting in maximum likelihood estimates. Introducing random effects to the model changes the way the likelihood function is computed. Only the distribution of the random effects are really interesting, but technically the individual η_i must be estimated for a set of parameters. Thus the optimisation turns into a two step optimisation procedure: The overall model parameters (population or first stage) and the individual (or second stage) parameters.

For a given set of population parameters the second stage optimisation identifies the η_i's for each subject. The numerical noise for the individual log-likelihood function is sufficiently small such that the gradient based quasi-Newton optimisation can be used. Each subject is independent and depending on the computer the speed of this part of the estimation can be significantly increased when running in parallel.

For this report 17 data sequences are used. Some of these data sequences came from the same person being studied over two different days. For now all trials are considered independent. The numerical noise from each of the 17 log-likelihood functions accumulate making the resulting population log-likelihood function quite noisy and unsuitable for a deterministic gradient based optimisation. The genetic algorithm is a stochastic optimiser which attempts to mimic evolution. An initial population is randomly drawn. A selection of the parameters yielding the best log-likelihood values breeds a new population. This process is continued until the fitness function does not improve over a period or when the computational budget is spend. For each of the three models, 1000 iterations are computed with a population of 50 resulting in 50.000 evaluations of the population log-likelihood. Each of them requires the second stage optimisation of the individual log-likelihood. The 1000 iterations take about 35 hours using 17 cores at the DTU High-Performance- Computing servers.

Details on the population log-likelihood can be found in [16]. Details on the individual log-likelihood can be found in [17].

3.6 Model Comparison

As the base model is nested into all the extended models, the models in Section 3.4 are compared to the base model in (2) and (3) by a likelihood-ratio-test (LRT). The likelihood ratio, λ_y, between two likelihoods can be written as:

$$\lambda_y = \log(L_{Ext}(\theta; y)) - \log(L_{Base}(\theta; y)) \tag{25}$$

where $L_{Ext}(\theta; y)$ and $L_{Base}(\theta; y)$ are the maximum likelihood estimates for the parameters θ given the data y of one of the extended models including exercise and the base model, respectively.

Under the null-hypothesis (claiming that the base model and the extended model perform equally), the random variable $-2\lambda(y)$ follows a $\chi^2_{(p-q)}$ distribution, where p and q are the number of the parameters in the base model and the extended model, respectively [21].

As the different models with an exercise extension are not nested, their performance is compared with Akaike Information Criteria (AIC) and Bayesian Information Criteria (BIC).

4 Results

Preliminary estimations showed that V_I was practically unidentifiable for the base model. Thus we fixed V_I for the rest of the study. The fixed parameters are seen in Table 1.

Table 1: *Value of fixed parameters*

Parameter	Value
S_{min}	0.438 [25]
V_I	0.19 [12]
Ip_{0i}	This value was fixed to the value of the first observation for each subject.

In the following, the three extended models will be evaluated.

4.1 Preliminary Model Evaluation

Initial estimations of *Model A* showed that the specification of k_a as an random walk was not appropriate. The variation in k_a was not significant. Thus this model was disregarded in the further evaluation.

4.2 Posterior Identifiability Check

The posterior identifiability is checked from the conditional likelihood profiles. They are computed for each estimated parameter by fixing all parameters except the parameter of interest and estimating the negative log-likelihood function. In Figure 2, the estimated profiles for the base model are seen. For all parameters except the variance of the measurement noise, S, the profile has a minimum. The same holds for *Model B* and *Model C* as seen in Figure 3 and 4.

The parameter estimates are within an acceptable range of the minimum for all parameters. The discrepancy between the estimate and the minimum of the curve for Ω_{Isc0} (the first element of the Ω matrix) in Figure 2 is caused by graphical issues. The curvature of the profiles around the minimum indicates the size of the uncertainty of the estimates. All three models seem to have a large uncertainty of $\hat{k}_e$ (ke.pop in the figures).

4.3 Model Comparison

The models are evaluated by comparing the maximum likelihood estimates with LRT, AIC and BIC. The estimates and the corresponding statistical measures can be seen in Table 2. As seen, *Model C* is assessed as the best model from all the criteria. Both *Model B* and *Model C* explain significantly more of the variability in the data than the base model.

Table 2: *Results of LRT, AIC and BIC*

Model	Number of estimated parameters	$-log(L)$	*p-value* from LRT	AIC	BIC
Base model	10	927	-	1878	1799
Model B	11	897	9.436896e-15	1817	1729
Model C	12	895	1.221245e-15	1815	1720

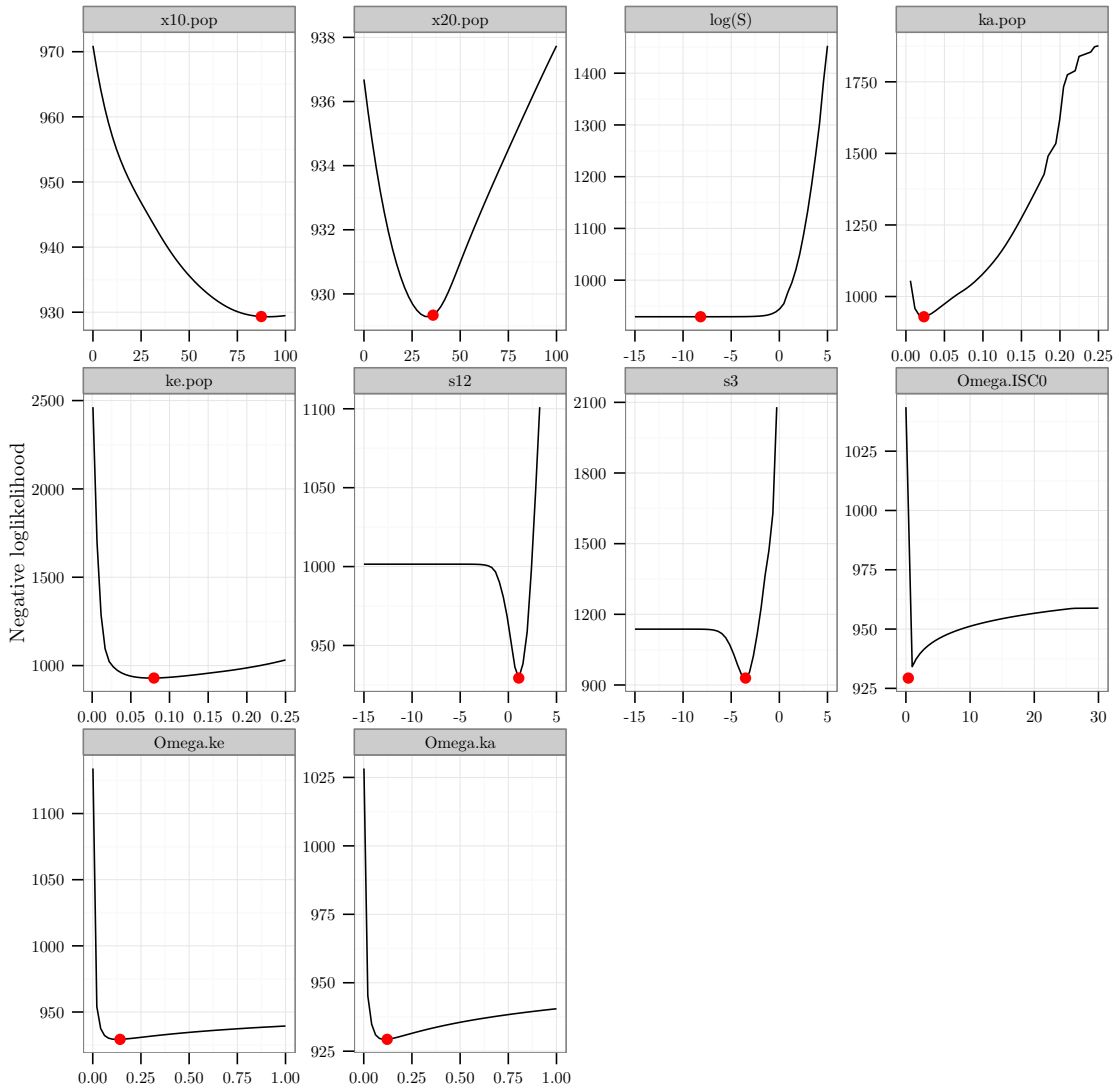

Figure 2: *Conditional loglikelihood profiles for the base model. The red points indicate the parameter estimates. x10.pop and x20.pop are the initial values of* Isc_1 *and* Isc_2*, respectively. S in the plot corresponds to* $\log(S)$ *in the model. ka.pop and ke.pop are* k_a *and* k_e*, respectively.* $s12 = \log(\sigma_{Isc})$ *and* $s3 = \log(\sigma_{Ip})$*. Omega.ISC0, Omega.ke, and Omega.ka are the diagonal elements of* Ω*.*

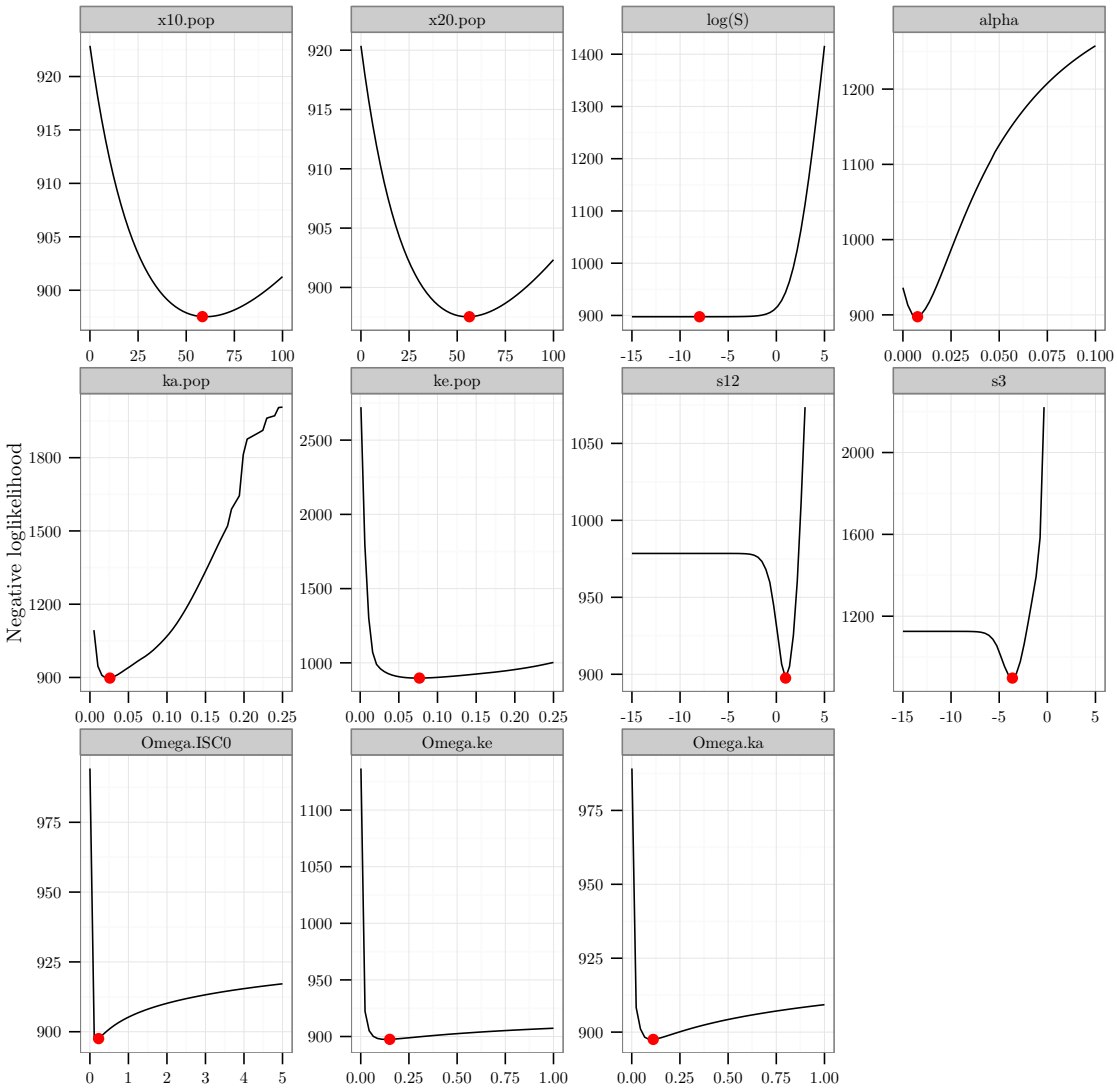

Figure 3: *Conditional loglikelihood profiles for Model B The red points indicate the parameter estimates. x10.pop and x20.pop are the initial values of* Isc_1 *and* Isc_2*, respectively. S in the plot corresponds to* $\log(S)$ *in the model .ka.pop and ke.pop are* $\bar{k}_a$ *and* k_e*, respectively.* $s12 = \log(\sigma_{Isc})$ *and* $s3 = \log(\sigma_{Ip})$*. Omega.ISC0, Omega.ke, and Omega.ka are the diagonal elements of* Ω*.*

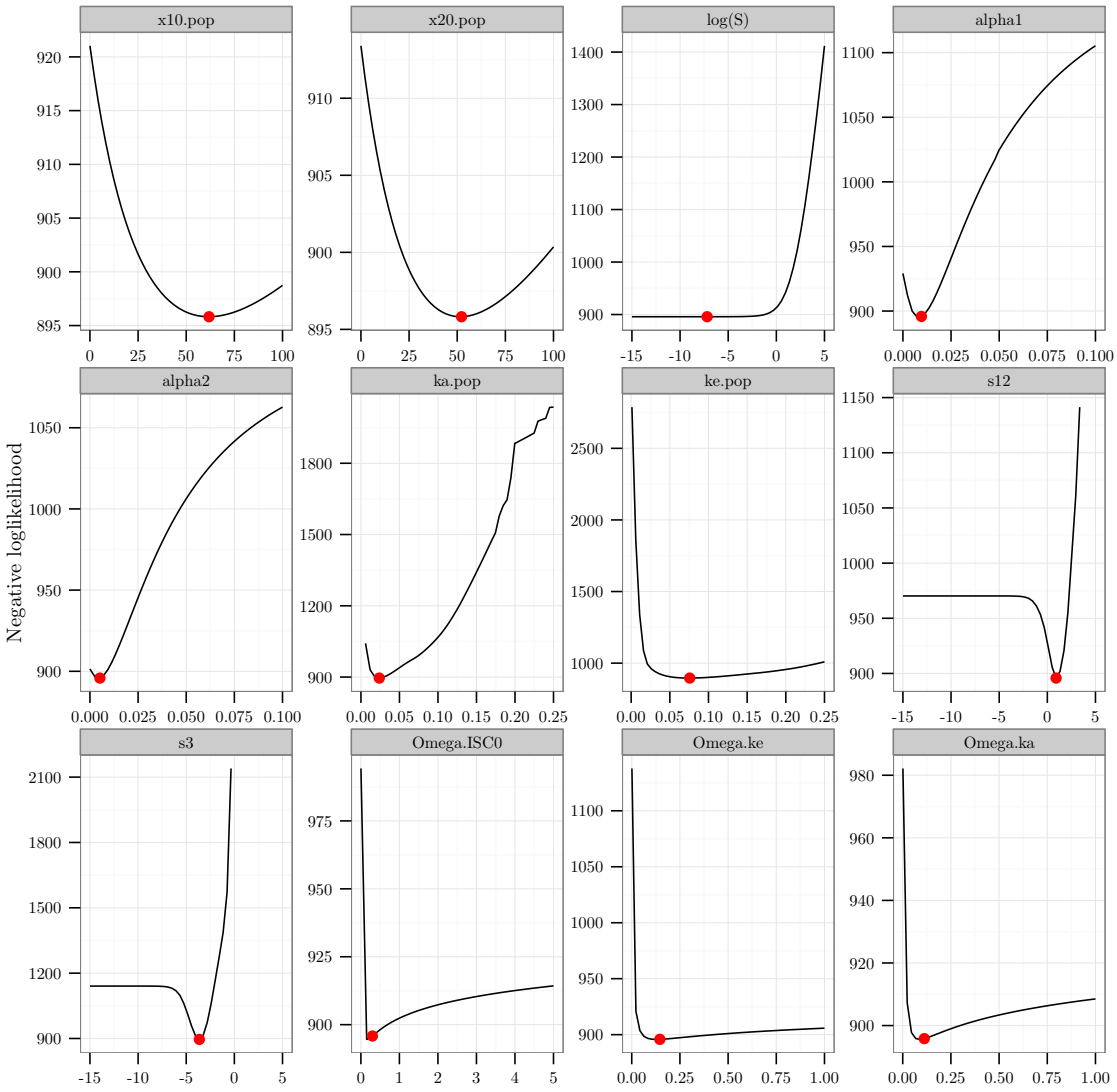

Figure 4: *Conditional loglikelihood profiles for Model C. The red points indicate the parameter estimates. x10.pop and x20.pop are the initial values of* Isc_1 *and* Isc_2*, respectively. S in the plot corresponds to* $\log(S)$ *in the model. ka.pop and ke.pop are* $\bar{k}_a$ *and* k_e*, respectively.* $s12 = \log(\sigma_{Isc})$ *and* $s3 = \log(\sigma_{Ip})$*. Omega.ISC0, Omega.ke, and Omega.ka are the diagonal elements of* Ω*.*

The parameter estimates for all three models are seen in Table 3. For *Model C*, the moderate intensity exercise results in a larger absorption rate than mild exercise.

Table 3: *Parameter estimates from the base model, Model B, and Model C*

	Base Model	*Model B*	*Model C*
Isc_{1_0}	87.4	58.3	61.8
Isc_{2_0}	35.9	56.3	52.2
k_a	0.023	0.026	0.024
k_e	0.079	0.077	0.076
σ_{Isc}	2.94	2.61	2.48
σ_{Ip}	0.030	0.027	0.026
S	0.000 28	0.000 34	0.000 75
Ω_{Isc}	0.379	0.226	0.299
Ω_{ka}	0.122	0.112	0.112
Ω_{ke}	0.142	0.150	0.146
α		0.007 62	
α_{mild}			0.009 61
$\alpha_{moderate}$			0.005 15

4.4 Model Predictions

From the above results, *Model C* with an intensity-dependent absorption rate is appointed as the best model to explain the dynamics. The one-step predictions from *Model C* for 3 representative data sequences are seen in Figure 5, 6 and 7. In general, the predictions are acceptable and the model does seem to capture the increase related to exercise. Especially, in Figure 7 the compliance between the predictions and the observations is good. The width of the prediction interval is however large in this case. The prediction in Figure 6 does not seem to follow the dynamics of the observations very well. The increase during exercise is underestimated and the increase due to the insulin bolus is overestimated. Finally, the prediction in Figure 6 underestimates the increase during exercise while the prediction of the bolus increase is acceptable.

4.5 Model Check

Diagnostic plots of the standardised residuals of *Model C* are depicted in Figure 8. Note that the initial value was fixed to the value of the first observations and thus the corresponding residual is equal to zero. The plots confirm that the model does not seriously violate the assumption of equally and normally distributed residuals.

5 Discussion

The purpose of this study is to evaluate three model extensions describing the relationship between exercise and the insulin absorption rate in CSII treated type 1 diabetes patients. From the model evaluations we appoint *Model C* as the best model extension. This model takes into account the intensity of the exercise bout. From a physiological point of view this is a reasonable hypothesis. The two separate terms for mild and moderate exercise could be replaced by the heart rate or percentage of maximum oxygen consumption.

During the estimation, seven of the 24 data sequences were disregarded due to non-steady initialization. The non-steady behavior could be caused by previously injected insulin in the early morning or changes in the basal delivery rate prior to study start. In future studies with these data, the observations from the initial stabilization period could be eliminated to avoid this problem. However, it is important to be

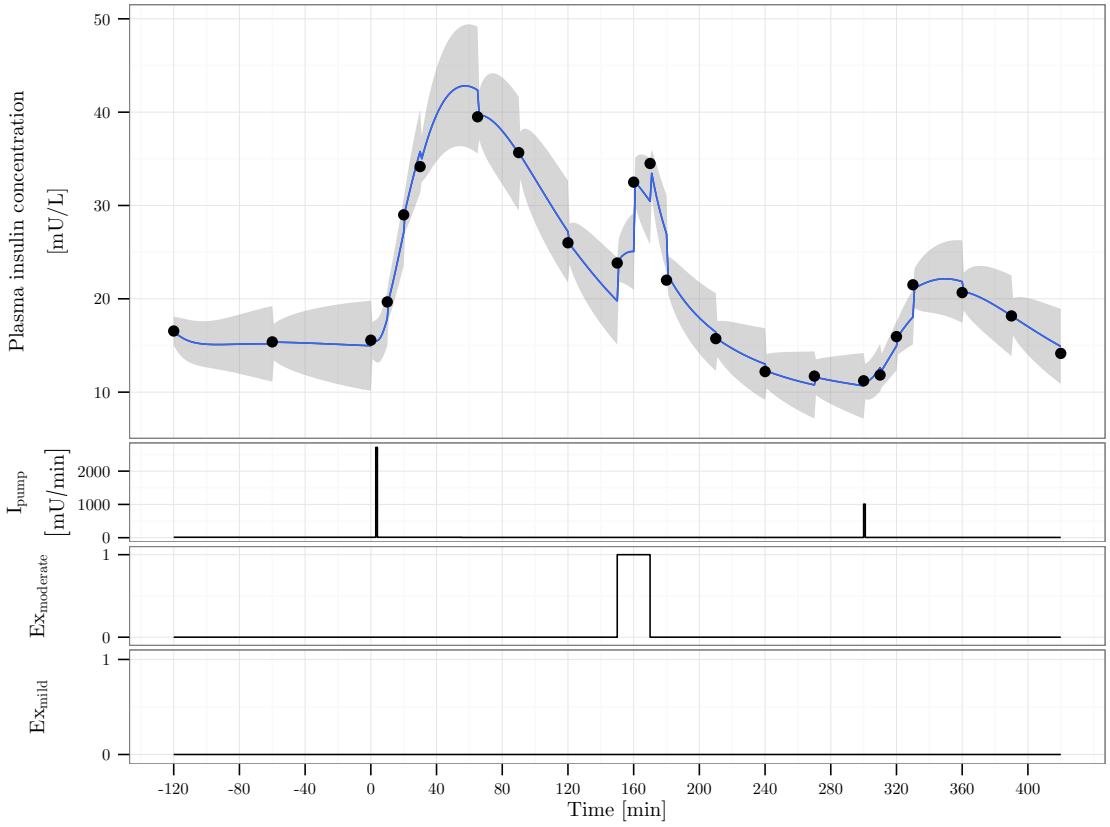

Figure 5: *Data sequence no. 8. Top: One-step predictions from Model C (Blue line). The observations are represented by dots. The grey area indicates 95% prediction interval. Middle and bottom: Insulin and exercise inputs.*

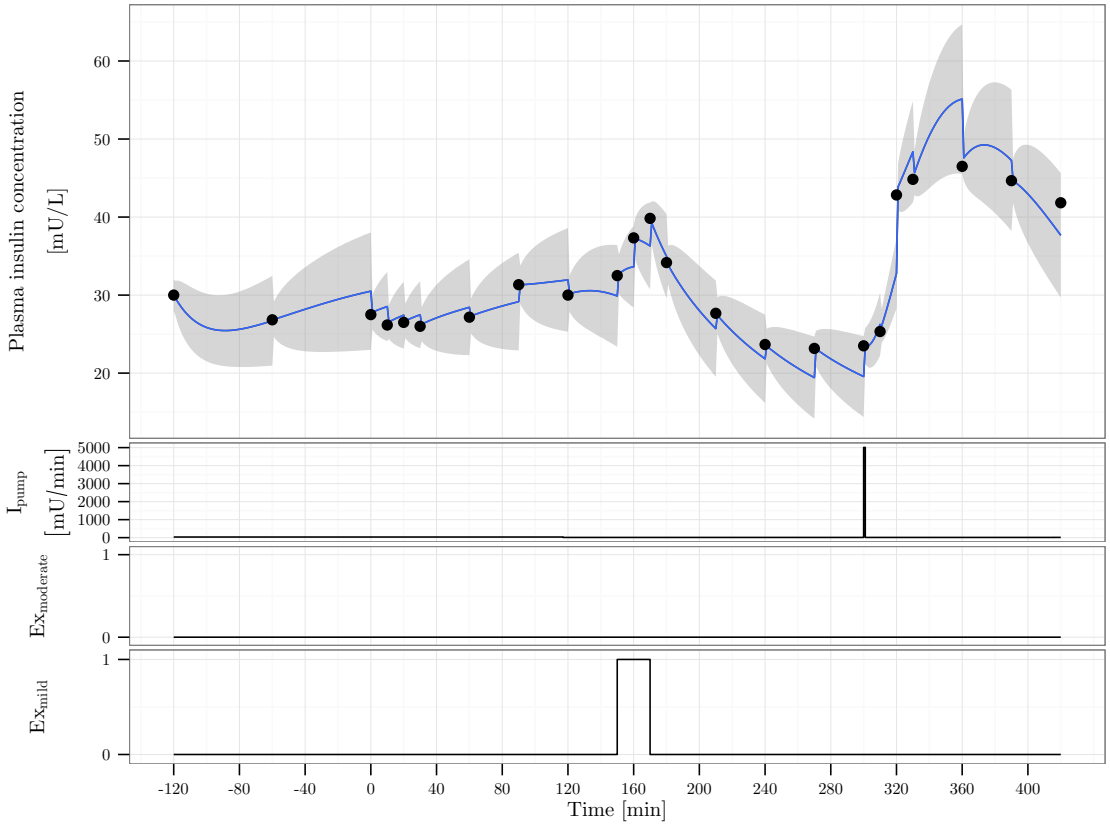

Figure 6: *Data sequence no. 9. Top: One-step predictions from Model C (Blue line). The observations are represented by dots. The grey area indicates 95% prediction interval. Middle and bottom: Insulin and exercise inputs.*

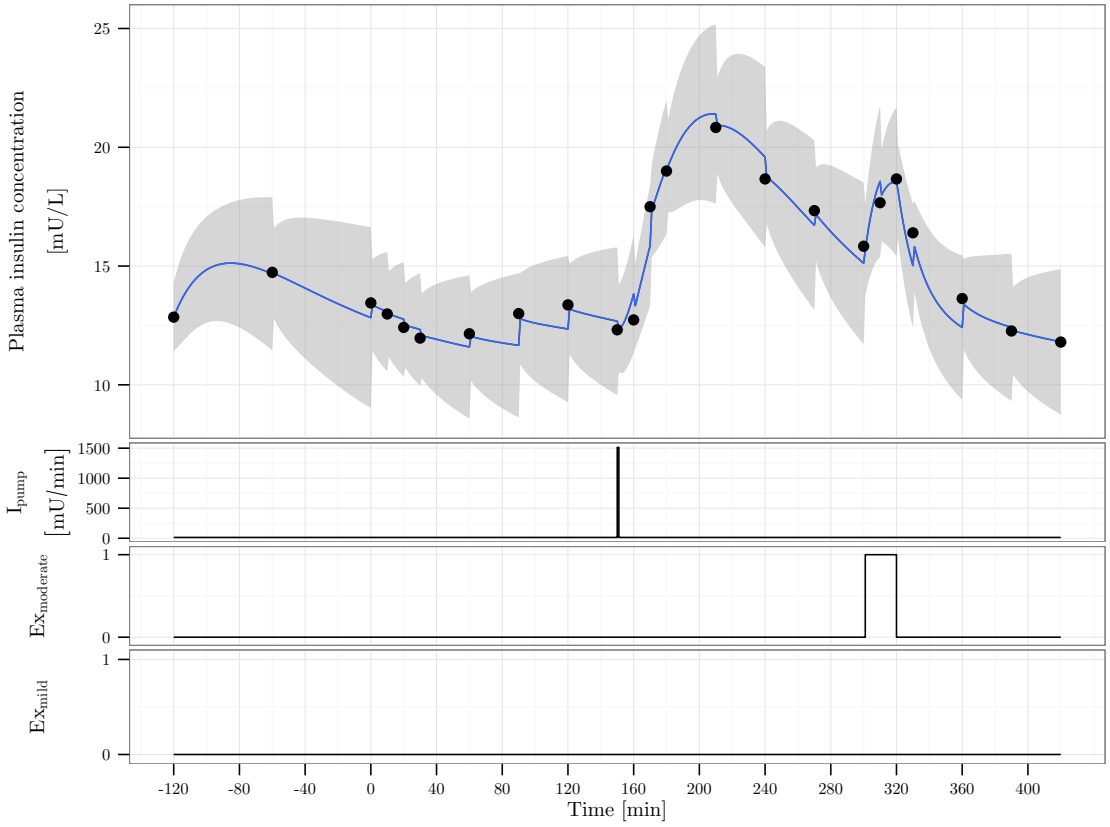

Figure 7: *Data sequence no. 10. Top: One-step predictions from Model C (Blue line). The observations are represented by dots. The grey area indicates 95% prediction interval. Middle and bottom: Insulin and exercise inputs.*

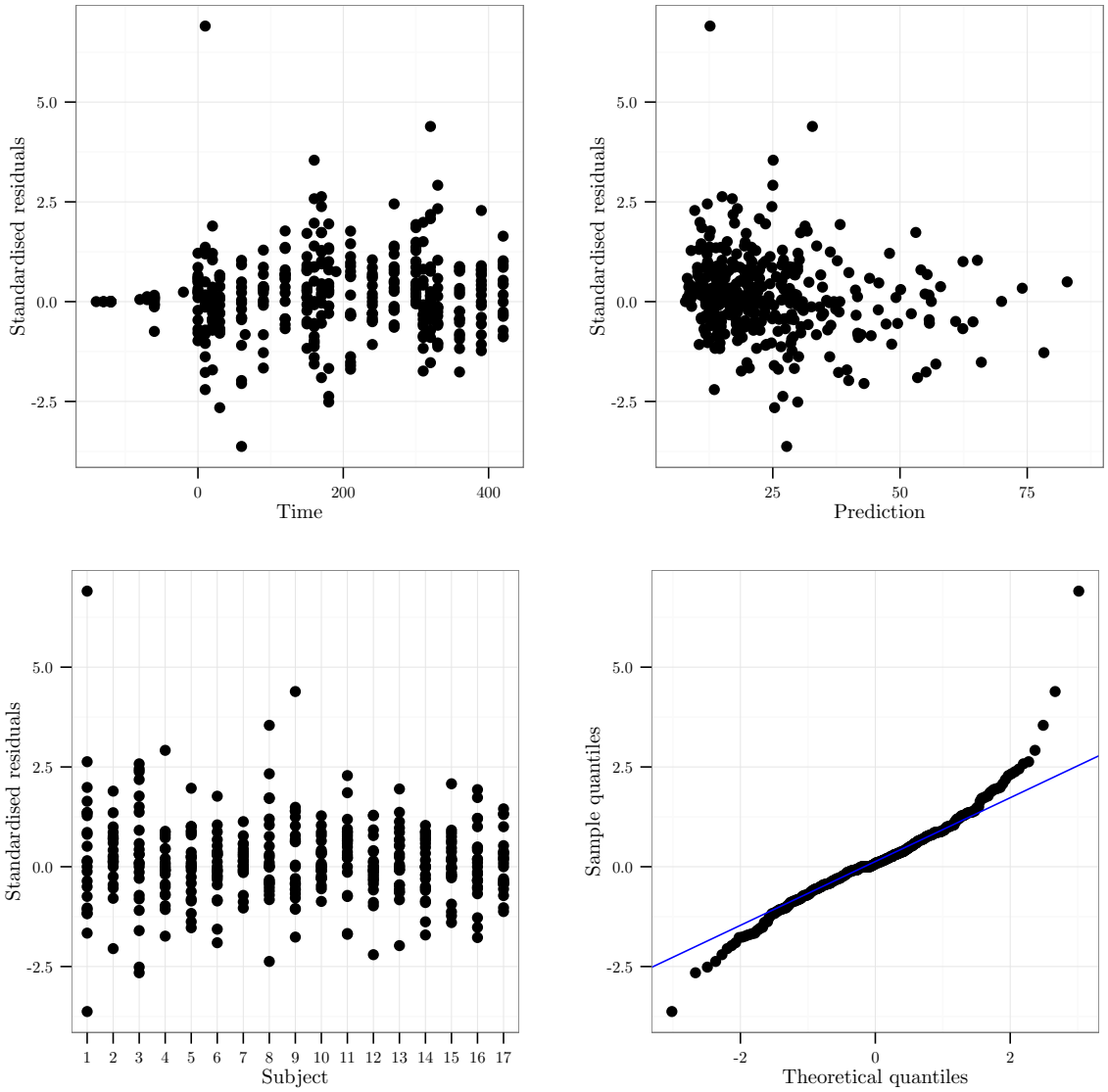

Figure 8: *Topleft: Standardised residuals versus time. Note that the initial value is fixed to the value of the first observations and thus the corresponding residual is equal to zero. Topright: Standardised residuals versus predictions. Bottomleft: Standardised residuals versus subjects (data sequences). Bottomright: QQ-plot of the standardised residuals versus a normal distribution.*

aware of any insulin boluses delivered during or in the hours prior to the stabilization period as some of the insulin would still be present in plasma at the time of the first event. Insulin is present in plasma upto 4-5 hours after the injection.

In the estimation, we have to assume that the data set was obtained from 17 individuals due to limitations in the software prototype. The original data set included 12 patients in total. Each patient went through two study days resulting in 24 data sequences. The 17 data sequences which were left after the initial data cleaning came from 10 patients. Thus we mix the inter-individual variability with the inter-occasion variability. In future versions of the software, the possibility to distinguish between these two variabilities is a necessity to ensure a correct handling of the variability.

The specification of the insulin absorption rate parameter k_a in *Model A* includes a random walk. This kind of parameter tracking is one of the main advantages of SDE models due to its ability to identify hidden relationships in the data. The random walk is predicted along with the other state predictions by a Kalman Filter. The data sequences included 23 observations each sampled non-equidistantly. The exercise bout lasted 20 minutes and plasma insulin was sampled at the start, after ten minutes, and at the end of the exercise bout. Thus, we had very few observations to drive the random walk. This could be the reason to the failure of *Model A*. Longer exercise bouts and very rich sampling are needed to use this method for model extension.

The clinical study investigated the effect of 20 minutes of exercise on a treadmill. Thus, the results cannot be extrapolated to other types of sport or other durations. Furthermore, the effect can be different for other types of insulin as well. To fully evaluate and model the effect of exercise on insulin kinetics in CSII treated type 1 diabetes patients, a clinical study designed to investigate this effect specifically is needed.

More complex models of the insulin pharmacokinetics have been proposed in the literature. In [35] 11 models were compared including the base model used here. The authors conclude that a more complex model is the most suitable model to explain the insulin dynamics. However, as the purpose of this study was to add complexity to the model, we prioritised to start with a simple model as base model.

The effect of exercise on the insulin absorption must be assumed to be exposed to inter-individual variability. Thus, the model fit would probably improve further by adding a random effect to α_{mild} and $\alpha_{moderate}$. This would likely improve the prediction of the increase in plasma insulin concentration during exercise, but as for the random walk in *Model A*, this extension would require longer time series to be identified.

As the software is a prototype, we cannot obtain the standard deviations of the parameters nor the covariances. Thus, the results are only tentative as we cannot fully validate the model. If we assume that the model is valid, the next step would be to perform covariate analysis to identify relationships between the individual η_i's and relevant covariates, e.g., age, level of fitness, weight, and gender.

The posterior identifiability check showed that for the base model, *Model B*, and *Model C* it is not possible to estimate a realistic variance of the measurement noise. This could indicate that the models are not able to fully capture the dynamics. Hence, the Kalman filter used in the estimation attempts to improve the fit by minimizing this variance.

The identified model has the potential to incorporated into a larger model of the insulin as well as glucose dynamics during exercise. The impact of the increased plasma insulin concentration on the plasma glucose concentration due to exercise still has to be investigated.

6 Conclusion

This study investigated the effect of exercise on the insulin absorption rate in CSII treated type 1 diabetes patients. Former models of exercise responses of the insulin-glucose system do not take this relationship into account. Three candidates for model extension of a population insulin pharmacokinetic model were evaluated. For all three models, the insulin absorption rate was assumed to be affected by exercise. In the first candidate, the absorption rate parameter was modelled as random walk. In this way, the model

structure was based completely on information from the data. However, as the data set did not include enough observations sampled during the exercise bout to drive the estimation, this model was disregarded. The two remaining models described a linear relationship between exercise and the absorption rate. One model included an absorption rate independent of intensity, and one included an intensity–dependent absorption rate. These two models were compared to a base model with a constant absorption rate with LRT, AIC and BIC. From these measures, the model with an intensity dependent absorption rate was evaluated as the best model to describe the data. A posterior identifiability check showed problems in estimating the variance of the measurement variance. The predictions from the best model showed that the model did capture behavior of the system and thus the model could be incorporated into an existing model of the insulin-glucose system in type 1 diabetes. Further clinical studies are needed to fully understand the increase in insulin plasma concentration during exercise. These studies should include dense sampling to allow for a fully data driven identification of an appropriate model.

References

[1] B. W. Bequette. Challenges and recent progress in the development of a closed-loop artificial pancreas. *Annual reviews in control*, 2012.

[2] M. Berger, H. Cüppers, H. Hegner, V. Jörgens, and P. Berchtold. Absorption kinetics and biologic effects of subcutaneously injected insulin preparations. *Diabetes Care*, 5(2):77–91, 1982.

[3] M. Berger, P. A. Halban, J.-P. Assal, R. Offord, M. Vranic, A. Renold, et al. Pharmacokinetics of subcutaneously injected tritiated insulin: effects of exercise. 1979.

[4] A. Breinholt, F. Ö. Thordarson, J. K. Møller, M. Grum, P. S. Mikkelsen, and H. Madsen. Grey-box modelling of flow in sewer systems with state-dependent diffusion. *Environmetrics*, 22(8):946–961, 2011.

[5] M. D. Breton. Physical activity – the major unaccounted impediment to closed loop control. *Journal of diabetes science and technology (Online)*, 2(1):169, 2008.

[6] C. Dalla Man, M. D. Breton, and C. Cobelli. Biosimulation modeling for diabetes: Physical activity into the meal glucose–insulin model of type 1 diabetes: In silico studies. *Journal of diabetes science and technology (Online)*, 3(1):56, 2009.

[7] C. Dalla Man, R. A. Rizza, and C. Cobelli. Meal simulation model of glucose-insulin system. *Conference proceedings : Annual International Conference of the IEEE Engineering in Medicine and Biology Society. IEEE Engineering in Medicine and Biology Society. Conference*, 1(10):307–10, jan 2007.

[8] M. Derouich and A. Boutayeb. The effect of physical exercise on the dynamics of glucose and insulin. *Journal of Biomechanics*, 35(7):911–917, 2002.

[9] DTU Compute, Technical University of Denmark. CTSM - Continuous time stochastic modelling in R, 2013.

[10] A. Duun-Henriksen, S. Schmidt, K. Nørgaard, and H. Madsen. Clinical data for advanced glucose modelling. Technical Report Technical Report-2013-06, DTU Compute, Technical University of Denmark, 2013.

[11] E. Fernqvist, B. Linde, J. Östman, and R. Gunnarsson. Effects of physical exercise on insulin absorption in insulin-dependent diabetics. a comparison between human and porcine insulin. *Clinical Physiology*, 6(6):489–497, 1986.

[12] A. Haidar, M. Wilinska, J. Graveston, and R. Hovorka. Stochastic virtual population of subjects with type 1 diabetes for the assessment of closed loop glucose controllers. 2013.

[13] M. Hernández-Ordoñez and D. Campos-Delgado. An extension to the compartmental model of type 1 diabetic patients to reproduce exercise periods with glycogen depletion and replenishment. *Journal of biomechanics*, 41(4):744–752, 2008.

[14] S. M. Iacus. Stochastic processes and stochastic differential equations. In *Simulation and Inference for Stochastic Differential Equations*, pages 1–59. Springer, 2008.

[15] S. S. Kanderian, S. Weinzimer, G. Voskanyan, and G. M. Steil. Identification of intraday metabolic profiles during closed-loop glucose control in individuals with type 1 diabetes. *Journal of diabetes science and technology*, 3(5):1047–57, Sep 2009.

[16] S. Klim, S. B. Mortensen, N. R. Kristensen, R. V. Overgaard, and H. Madsen. Population stochastic modelling (PSM)–an R package for mixed-effects models based on stochastic differential equations. *Computer methods and programs in biomedicine*, 94(3):279–289, 2009.

[17] N. R. Kristensen, H. Madsen, and S. B. Jørgensen. Parameter estimation in stochastic grey-box models. *Automatica*, 40(2):225–237, 2004.

[18] P. J. Lenart and R. S. Parker. Modeling exercise effects in type i diabetic patients. In *World Congress*, volume 15, pages 1348–1348, 2002.

[19] H. Madsen. *Time Series Analysis*. Chapman & Hall/CRC, 2008.

[20] H. Madsen and J. Holst. Modelling non-linear and non-stationary time series. *Lecture Notes, Technical University of Denmark, Dpt. of Informatics and Mathematical Modeling, Kgs. Lyngby, Denmark*, 2000.

[21] H. Madsen and P. Thyregod. *Introduction to general and generalized linear models*. CRC Press, 2011.

[22] R. R. Meldgaard. Stochastic differential equations in pharmacokinetic/pharmacodynamic modelling. Master's thesis, Technical University of Denmark, Kgs. Lyngby, Denmark, 2011.

[23] J. K. Møller, J. Carstensen, and H. Madsen. Structural identification and validation in stochastic differential equation based models-with application to a marine ecosystem np-model. *Journal of the Royal Statistical Society, Series C*, 2011.

[24] J. K. Møller and H. Madsen. From state dependent diffusion to constant diffusion in stochastic differential equations by the lamperti transform. Technical report, DTU Informatics, Building 321, 2010.

[25] S. B. Petersen, J. M. Lovmand, L. Honoré, C. B. Jeppesen, L. Pridal, and O. Skyggebjerg. Comparison of a luminescent oxygen channeling immunoassay and an ELISA for detecting insulin aspart in human serum. *Journal of Pharmaceutical and Biomedical Analysis*, 51(1):217–224, 2010.

[26] A. Roy, R. S. Parker, et al. Dynamic modeling of exercise effects on plasma glucose and insulin levels. *Journal of Diabetes Science and Technology*, 1(3):338–347, 2007.

[27] S. Schmidt, D. A. Finan, A. K. Duun-Henriksen, J. B. Jørgensen, H. Madsen, H. Bengtsson, J. J. Holst, S. Madsbad, and K. Nørgaard. Effects of everyday life events on glucose, insulin, and glucagon dynamics in continuous subcutaneous insulin infusion–treated type 1 diabetes: collection of clinical data for glucose modeling. *Diabetes technology & therapeutics*, 14(3):210–217, 2012.

[28] G. Sonnenberg, F. Kemmer, and M. Berger. Exercise in type 1 (insulin-dependent) diabetic patients treated with continuous subcutaneous insulin infusion. *Diabetologia*, 33(11):696–703, 1990.

[29] H. Süsstrunk, B. Morell, W. Ziegler, and E. Froesch. Insulin absorption from the abdomen and the thigh in healthy subjects during rest and exercise: blood glucose, plasma insulin, growth hormone, adrenaline and noradrenaline levels. *Diabetologia*, 22(3):171–174, 1982.

[30] J. Thow, A. Johnson, M. Antsiferov, and P. Home. Exercise augments the absorption of isophane (nph) insulin. *Diabetic medicine*, 6(4):342–345, 1989.

[31] C. Tonoli, E. Heyman, B. Roelands, L. Buyse, S. S. Cheung, S. Berthoin, and R. Meeusen. Effects of different types of acute and chronic (training) exercise on glycaemic control in type 1 diabetes mellitus. *Sports Medicine*, 42(12):1059–1080, 2012.

[32] C. W. Tornøe, R. V. Overgaard, H. Agersø, H. A. Nielsen, H. Madsen, and E. N. Jonsson. Stochastic differential equations in NONMEM: implementation, application, and comparison with ordinary differential equations. *Pharmaceutical research*, 22(8):1247–58, Aug 2005.

[33] J. J. Valletta, A. J. Chipperfield, and C. D. Byrne. Gaussian process modelling of blood glucose response to free-living physical activity data in people with type 1 diabetes. In *Engineering in Medicine and Biology Society, 2009. EMBC 2009. Annual International Conference of the IEEE*, pages 4913–4916. IEEE, 2009.

[34] M. E. Wilinska, L. J. Chassin, C. L. Acerini, J. M. Allen, D. B. Dunger, and R. Hovorka. Simulation environment to evaluate closed-loop insulin delivery systems in type 1 diabetes. *Journal of diabetes science and technology*, 4(1):132–44, Jan 2010.

[35] M. E. Wilinska, L. J. Chassin, H. C. Schaller, L. Schaupp, T. R. Pieber, and R. Hovorka. Insulin Kinetics in Type-1 Diabetes: Continuous and Bolus Delivery of Rapid Acting Insulin. 52(1):3–12, 2005.

[36] B. Zinman, M. Vranic, A. M. Albisser, B. S. Leibel, and E. B. Marliss. The role of insulin in the metabolic response to exercise in diabetic man. *Diabetes*, 28(Supplement 1):76–81, 1979.